Tuning the temperature range of superelastic Ni-Ti alloys for elastocaloric cooling via thermal processing

Journal of Physics: Energy

PAPER

Tuning the temperature range of superelastic Ni-Ti alloys for elastocaloric cooling via thermal processing

Takahiro Yamazaki[1,2,*], Andre L Montagnoli[3], Marcus L Young[3] and Ichiro Takeuchi[2,*]

[1] Department of Materials Science and Technology, Tokyo University of Science, Katsushika, Tokyo 125-8585, Japan
[2] Department of Materials Science and Engineering, The University of Maryland, College Park, MD 20742, United States of America
[3] Department of Materials Science and Engineering, University of North Texas, Denton, TX 76207, United States of America
[*] Authors to whom any correspondence should be addressed.

E-mail: tyamazak@umd.edu and takeuchi@umd.edu

Keywords: elastocaloric cooling, superelasticity, Ni-Ti shape memory alloy, austenite finish temperature, thermal processing

OPEN ACCESS

RECEIVED
29 January 2023

REVISED
27 March 2023

ACCEPTED FOR PUBLICATION
14 April 2023

PUBLISHED
28 April 2023

Abstract

Caloric cooling enlisting solid-state refrigerants is potentially a promising eco-friendly alternative to conventional cooling based on vapor compression. The most common refrigerant materials for elastocaloric cooling to date are Ni-Ti based superelastic shape memory alloys. Here, we have explored tuning the operation temperature range of $Ni_{50.8}Ti_{49.2}$ for elastocaloric cooling. In particular, we have studied the effect of thermal treatments (a.k.a. aging) on the transformation temperature, superelasticity, and elastocaloric effects of $Ni_{50.8}Ti_{49.2}$ shape memory alloy tubes. The isothermal compressive test revealed that the residual strain of thermally-treated Ni-Ti tubes at room temperature approaches zero as aging time is increased. Short-time aging treatment at 400 °C resulted in good superelasticity and elastocaloric cooling performance with a large tunable austenite finish (A_f) temperature range of 24.7 °C, as determined from the A_f temperature of the samples that were aged 5–120 min. The main reason of the property change is the formation of a different amount of Ni_4Ti_3 precipitates in the NiTi matrix. Our findings show that it is possible to tailor the A_f temperature range for development of cascade elastocaloric cooling systems by thermally treating a starting single composition Ni-Ti alloy.

1. Introduction

Elastocaloric cooling is attracting attention as an alternative eco-friendly cooling technique with potentials to be comparable in efficiency to conventional vapor compression [1–4]. It is based on the elastocaloric effect, where uniaxial stress applied to a superelastic material leads to release and then absorption of latent heat associated with a phase transition. Ni-Ti alloys are versatile shape memory alloys which have been implemented for a variety of applications, including medical stents, vibration dampers for aircrafts, and now the elastocaloric effect [2]. The unique elastocaloric behavior of Ni-Ti is based on its thermoelastic phase transformation. In order to continue the development of cooling devices based on the elastocaloric effect, it is important to explore how the properties of Ni-Ti can be tuned [1, 3]. In particular, it is imperative to implement elastocaloric materials whose optimum operating temperatures are properly tuned for the development of cascade regenerators [5, 6].

To date, there have been many studies on the metallographic features of binary Ni-Ti alloys, which are delicately sensitive to the average composition and annealing conditions [7, 8]. It is well-known that the martensitic transformation temperature in Ni-Ti shape memory alloys can be adjusted by over 100 °C by incorporating appropriate third elements [7–11]. Frenzel *et al*, have demonstrated that a 1% change in the Ni concentration can change the transformation temperature by over 100 °C [8]. Also, while the nominal 50 at% Ni nitinol (NiTi) has an austenitic transformation finish A_f temperature close to room temperature, the A_f temperature can be lowered by 100 °C by adding 4 at% of V (vanadium), or increased by as much as 150 °C by adding 15 at% of Hf (hafnium) [7]. Such a significant degree of transition temperature tunability is not achievable in other caloric materials.

According to the stress-temperature diagram of Ni-Ti alloys [12], the critical stress to induce superelastic transformation plays an important role in elastocaloric properties. In particular, the thermomechanical properties can be maximally utilized by setting the austenite finish (A_f) temperature to be slightly lower than the ambient temperature [13, 14]. In multi-stage caloric cascade regenerators, where the goal is to establish a giant temperature lift (ΔT) across the regenerators, it is desirable to implement different elastocaloric materials whose A_f temperatures are varied from stage to stage. This idea is borrowed from magnetocaloric cascade regenerators whose refrigerants in successive stages have continuously tuned transformation temperatures (Curie temperatures) [15]. In a direct analogy, therefore, it is desirable to have Ni-Ti-based alloys whose A_f temperatures are tunable.

The thermomechanical picture of Ni-Ti, including the influence of the microstructure on A_f temperature, is complex because of the metallographic intricacies of Ni-Ti alloys [12, 16]. On the other hand, heat treatments can enable control of the transformation temperatures of bulk Ni-Ti alloys in a straightforward manner. Therefore, tailoring thermal process procedures for Ni-Ti might provide a way to help construct an elastocaloric device having multi-A_f solid-state refrigerants. Based on the equivalent phase diagram [8] and time–temperature–transformation (TTT) diagram [12], superelastic Ni-Ti alloys have been investigated to improve the shape memory effect and superelastic properties [14, 17]. However, the appropriate aging treatment of Ni-Ti alloys to improve elastocaloric effects has not been fully understood.

While large tunability via controlled introduction of a third element is attractive from a materials design point of view, they represent complexities in composition control, leading to possible additional manufacturing challenges of the overall regenerators. Thus, in this study, we opted to focus on establishing thermal processing techniques for systematically tuning the A_f temperature from a single type of superelastic Ni-Ti alloy. To accomplish this goal, commercial $Ni_{50.8}Ti_{49.2}$ alloy tubes were subjected to various thermal treatments such as annealing and low-temperature aging processes, and the subsequent isothermal/adiabatic mechanical responses were investigated. This study presents the results of the influence of these treatments on the crystal structure, transformation temperatures, isothermal superelastic properties, and adiabatic elastocaloric effect of Ni-Ti tubes.

2. Experimental

2.1. Sample preparation

Commercially available $Ni_{50.8}Ti_{49.2}$ (at%) alloy tubes (SE508, Confluent Medical Technologies) were used in this study. The sample geometry is a thin-walled tube with an inner diameter of 3.75 mm, an outer diameter of 4.72 mm, and a height of 20.0 mm, as shown in figure 1(a). The thin-walled tube used in this study possesses a large volume-to-surface ratio, which is ideal from the perspective of the heat exchange process and crucial for solid-state refrigerant applications [2].

Various thermal processing involving systematic variations in time and temperature were conducted based on the phase diagram of Ni-Ti as shown in figure 2. The samples were initially annealed at 900 °C–1000 °C for 60 min and subsequently quenched into a water bath as a homogenizing (solution) treatment. Here, it should be noted the quenching temperature of 900 °C and 1000 °C was high enough for homogenization of Ni-Ti according to solid-solution region in Ni-Ti phase diagram [9]. The first group of samples was then annealed for various aging periods ranging from 5 to 120 min at 400 °C (which we refer to as the aging treatment). The second group of samples was subjected to various aging temperatures ranging from 400 °C to 700 °C for 60 min (annealing treatment). After annealing, the samples in both groups were quenched into a water bath again. These heat treatments were performed in a quartz tube filled with argon gas.

2.2. Evaluation of austenite-martensite transformation temperatures

The austenite (B2)—martensite (B19′) phase transformation temperature was evaluated by differential scanning calorimetry (DSC; Q100, TA instruments) operated from −80 to 80 °C at the cooling/heating rate of 10 °C min^{-1}. Each measurement was conducted for two cycles in a flowing nitrogen gas atmosphere at 50 ml min^{-1}. The specimens were cut into small pieces (20–40 mg) from the edge of the tube sample. The transformation start/finish temperatures in the cooling and heating processes (M_s, M_f, A_s, and A_f) and the latent heat ($\Delta H_{A \to M}$ and $\Delta H_{M \to A}$) unit per weight were determined from the DSC curves.

2.3. Crystal structure analysis

The crystal structure and the formation of Ni-rich intermetallic phases were identified using an x-ray micro diffractometer (μXRD) (RINT-RAPID-S, Rigaku), with Cu-kα radiation of 1.5418 Å. The specimen was cut from a small piece of Ni-Ti tube, and it was measured with a collimator size of 0.3 mm and an imaging plate.

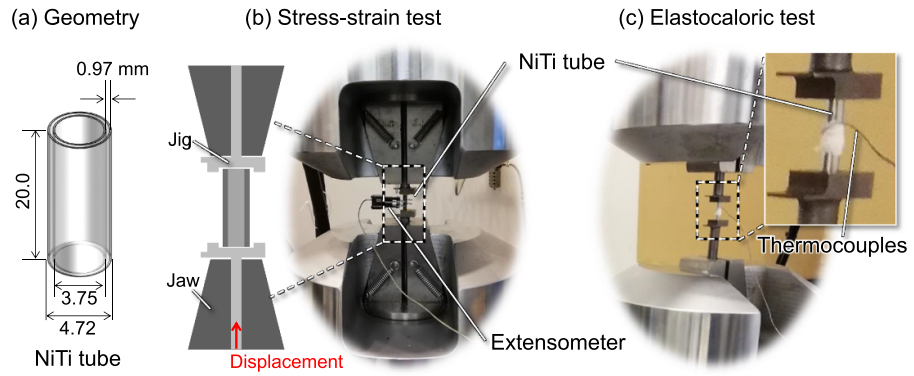

Figure 1. (a) The geometry of the Ni-Ti tube and the experimental setup for (b) compressive stress–strain mechanical test with the extensometer and (c) elastocaloric test with thermocouples.

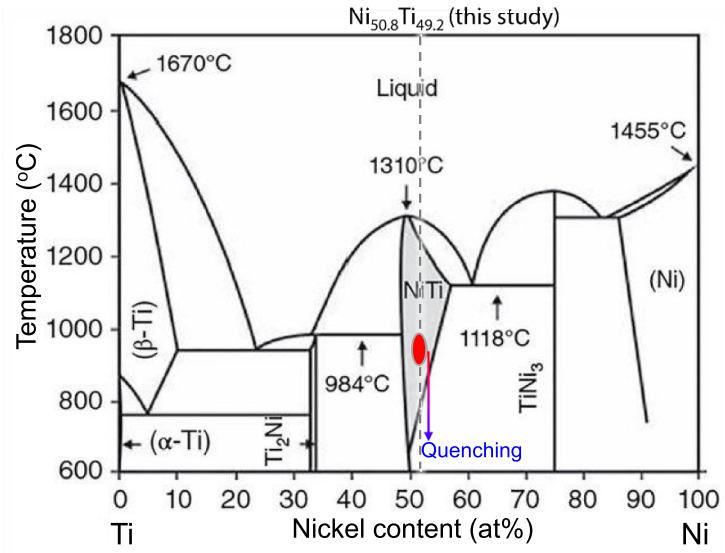

Figure 2. Phase diagram of Ni-Ti alloy with the highlighted NiTi single-phase (B2). Reprinted from [9], Copyright (2010), with permission from Acta Materialia Inc. Published by Elsevier Ltd.

Then, using 2D data processing software 2DP (Rigaku), pre-processing, such as 1D conversion, background subtraction, and smoothing, was carried out to identify the crystal structure contributing to the enhancement of the thermomechanical response.

2.4. Compressive stress–strain tests

The superelasticity of Ni-Ti tubes was evaluated under isothermal cyclic tests using an MTS 810 hydraulic universal testing machine with an axial extensometer (Model 632.26, MTS systems). The compressive stress–strain response was controlled by the displacement in the loading/unloading process at room temperature (∼20 °C), as shown in figure 1(b). The mechanical response was evaluated by continuously applying 2%–7% displacement to the sample at a strain rate of 0.02 s^{-1}. As a superelastic property, the strain energy (E_ε) was measured from the stress–strain loop of 7%-displacement-based strain, and the residual strain (ε_{res}) was determined after the last cyclic test. Displacement calibration was conducted before each measurement, and each stress–strain curve was run for five cycles.

2.5. Adiabatic temperature changes measurements

To evaluate the elastocaloric effect, compression cycle tests were conducted under an adiabatic loading and unloading condition in continuous operation at 1 Hz. Each stress–strain curve was run for four cycles under a range of displacement-based strains from 2%–7% at a strain rate of 0.2–0.7 s^{-1}. The temperature changes/lifts during the heating and cooling process (ΔT_h, ΔT_c) were obtained using T-type thermocouples, which were calibrated against a P795 resistance temperature detector. Post-displacement calibration was

performed before each measurement, while no pre-training was conducted. A holding period of 180 s was allotted to ensure that the temperature had returned to ambient and was stable after each loading/unloading process.

3. Results and discussion

3.1. Tuning A_f temperature via aging treatment

Figure 3 shows the DSC curves of Ni-Ti alloys undergoing various aging treatments for the first group of samples (homogenized first and then aged at 400 °C) with different durations ranging from 5 to 120 min. The vertical axis indicates the heat flow as a function of time, with convex upper graphs representing exothermic reactions and convex lower graphs representing endothermic reactions. Table 1 presents the transformation temperatures and latent heat per unit weight of the thermally-treated Ni-Ti alloys during the heating and cooling processes for both groups of samples.

We found that both transformation start/finish temperatures and the latent heat of Ni-Ti alloys systematically increased with increasing aging time periods in the range of 5–120 min. Notably, the A_f temperature, which is a key parameter for determining the elastocaloric cooling operation temperature, was observed to be near room-temperature (21.2 °C) for a 10 min aged sample. The maximum A_f temperature of 45.9 °C was observed for the sample aged for 120 min. The DSC curve for the sample aged for 30–120 min during the cooling process exhibits a double peak, indicating the two-stage transformation of martensite (B19′)—R-phase—austenite (B2), which is the intermediate phase generated during martensitic transformation. The R-phase generated during the multi-stage martensitic transformation has been attributed to the formation of Ni_4Ti_3 precipitates during aging treatments [18, 19].

Figure 4 shows the dependence of A_f temperature on the aging time at 400 °C (first group) and annealing temperature (second group). The results of DSC analysis indicated that A_f temperature increased rapidly with the aging time period, saturating at approximately 45 °C after 120 min. This is attributed to the formation of a metastable phase compound in the aging process, which alters the Ni concentration and, as a result, A_f temperature [9]. Furthermore, the A_f temperature dropped sharply with the annealing treatment at temperatures above 500 °C and remained constant for processing temperatures between 600 °C–700 °C. These changes of both A_f and M_f temperatures are consistent with previous studies [20–24]. These A_f temperature behavior are similar in terms of function of annealing temperature to a previous work by Feng *et al*, which showed that the transformation temperatures increased when annealed at a lower temperature (i.e. 350 °C–450 °C) [25] and it decreased when annealed at a relatively higher temperature (i.e. 550 °C–650 °C) [23, 25]. Also, the increase of A_f in the annealing temperature range of 600 °C–700 °C is consistent with the findings reported by Xu *et al* [22].

The latent heat $\Delta H_{M\rightarrow A}$, which is an important parameter for the elastocaloric effect, showed a peak value of 17.6 J g^{-1} for the 650 °C/60 min samples, and it decreased with the increase of annealing temperature (figure 4(f)). In terms of the A_f temperature for these samples, it appears to be optimal for the samples aged at 400 °C for 5–10 min and annealed at 500 °C–550 °C for achieving elastocaloric materials for operation near room temperature. However, several studies revealed that superelastic properties, especially the recoverable and plateau stresses of Ni-Ti wires annealed at temperatures above around 500 °C–600 °C, decreased significantly, likely due to the plastic deformation of the austenite phase occurring before the stress-induced martensite transformation or due to the formation of large Ni_4Ti_3 precipitates in the NiTi matrix [20, 26, 27]. It also should be noted that we might have achieved optimal A_f temperature, but not necessarily optimal fatigue behavior depending on the size, morphology, and distribution of the precipitates. The elastocaloric behavior also depends on these nano-scale features, but indirectly. Therefore, a further study on the influence of aging treatment at relatively low temperatures on superelasticity and elastocaloric effects with a focus on the microstructure is in order.

3.2. Crystal structure characterization

The crystal structure was analyzed to gain insight into the metallurgical origin of significant superelasticity and the elastocaloric effect following the thermal processing. Figure 5 illustrates the XRD 2D images and 1D patterns for the homogenized and aged samples. The μXRD results indicated that the Ni-Ti specimens possessed a polycrystalline texture with submicron grains. The XRD patterns showed that the homogenized sample was composed of a single phase of Ni-Ti matrix, and the other samples consisted of the Ni-Ti matrix and additional Ni-rich intermetallic phases, such as Ni_4Ti_3, Ni_3Ti_2, and Ni_3Ti, which are consistent with previous literature [8, 28, 29]. As the duration of low-temperature aging is increased, Ni_4Ti_3 phase was formed in the 10 min-aged samples, and Ni_3Ti_2 and Ni_3Ti phases were formed in the sample aged for over

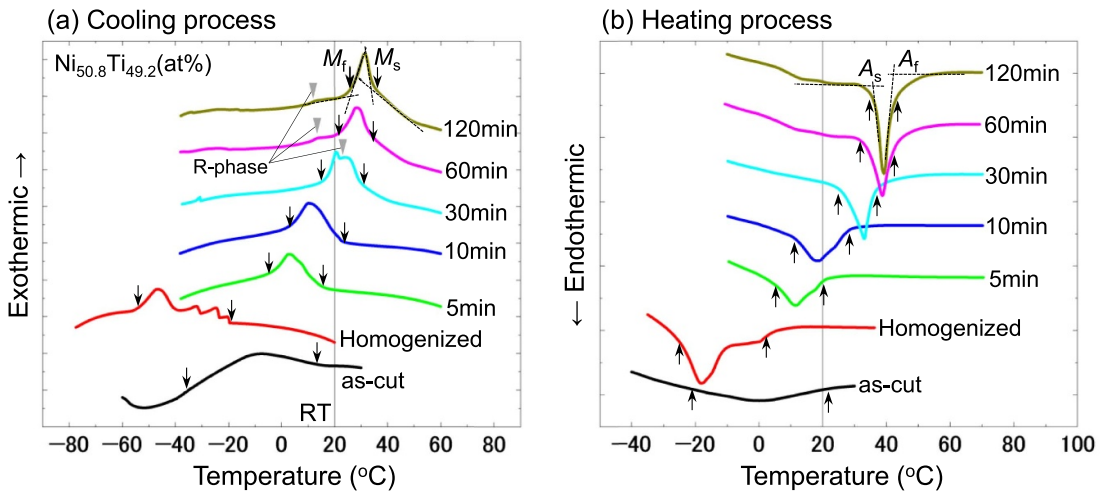

Figure 3. DSC curves for (a) heating and (b) cooling processes with the austenite-martensite transformation of superelastic Ni-Ti alloys in as-cut, homogenized and aged for 5, 10, 30, 60, and 120 min at 400 °C.

Table 1. Austenite-martensite transformation temperature and latent heat for thermally-treated Ni-Ti alloys.

		Cooling process			Heating process		
	Samples	M_s (°C)	M_f (°C)	$\Delta H_{A\to M}$ (J g^{-1})	A_s (°C)	A_f (°C)	$\Delta H_{M\to A}$ (J g^{-1})
	as-cut	13.7	−38.8	2.6	−20.6	22.2	3.5
	Homogenized	−19.6	−54.1	3.8	−26.2	5.1	8.3
Group 1[a]	400 °C/5 min	13.6	−2.7	2.9	3.6	21.2	3.1
	400 °C/10 min	21.5	3.5	3.7	10.2	28.2	3.5
	400 °C/30 min	30.8	16.9	4.0	26.3	36.8	4.6
	400 °C/60 min	33.2	22.4	4.9	33.2	43.7	5.2
	400 °C/120 min	35.7	26.7	5.9	35.6	45.9	5.5
Group 2[a]	500 °C/60 min	17.0	−26.9	5.3	22.3	32.4	12.0
	550 °C/60 min	−7.9	−31.6	14.2	5.7	18.0	17.6
	600 °C/60 min	−29.7	−47.4	5.9	−5.0	−19.8	7.7
	650 °C/60 min	−25.1	−43.5	6.8	0.2	−15.0	7.7
	700 °C/60 min	−25.6	−41.0	6.5	−5.6	−15.2	8.1

[a] Group 1 was homogenized first at 1000 °C and then samples underwent aging at 400 °C for specified periods. Group 2 was homogenized at 900 °C and treated at the specified temperatures for 60 min.

30 min. The formation of these phases is in agreement with the results of previous studies on the relationship between thermal processing and microstructure [30]. This dependence on aging time is attributed to the evolution of the density and size of Ni_4Ti_3 precipitates. Based on the TTT diagram [16], the formation of nano-Ni_4Ti_3 precipitates has previously been confirmed by Transmission electron microscopy (TEM) diffraction images in the aging effect at low temperatures around 250 °C–400 °C [18].

Surikov *et al* reported that the introduction of nano-Ti_4Ni_3 precipitates smaller than 10 nm into the matrix phase of NiTi improves superelasticity [31] and allows for the tuning of the transformation temperatures due to composition changes [32]. They furthermore confirmed that both Ni_4Ti_3 and Ni_3Ti_2 phases are intermediate phases, and the diffusional transformations occur in the following order with increasing aging temperature and time, Ni_3Ti being the equilibrium phase: metastable Ni_4Ti_3 → metastable Ni_3Ti_2 → stable Ni_3Ti. At lower aging temperatures and shorter aging time periods, the Ni_4Ti_3 phase appears. Conversely, at higher aging temperatures and longer aging periods, the Ni_3Ti phase appears, and at intermediate temperatures and times, the Ni_3Ti_2 phase appears [25]. They also observed that by prolonging aging, the preexisted Ni_4Ti_3 phase is absorbed in the matrix, leading to an increase in density and the size of the Ni_3Ti_2 phase.

It has been reported that precipitation hardening caused by the precipitation of Ni_4Ti_3 produced by the age-hardening treatment contributes to the improvement of superelasticity by making the alloy less susceptible to slip [28]. These results revealed that it is important to control the microstructures and

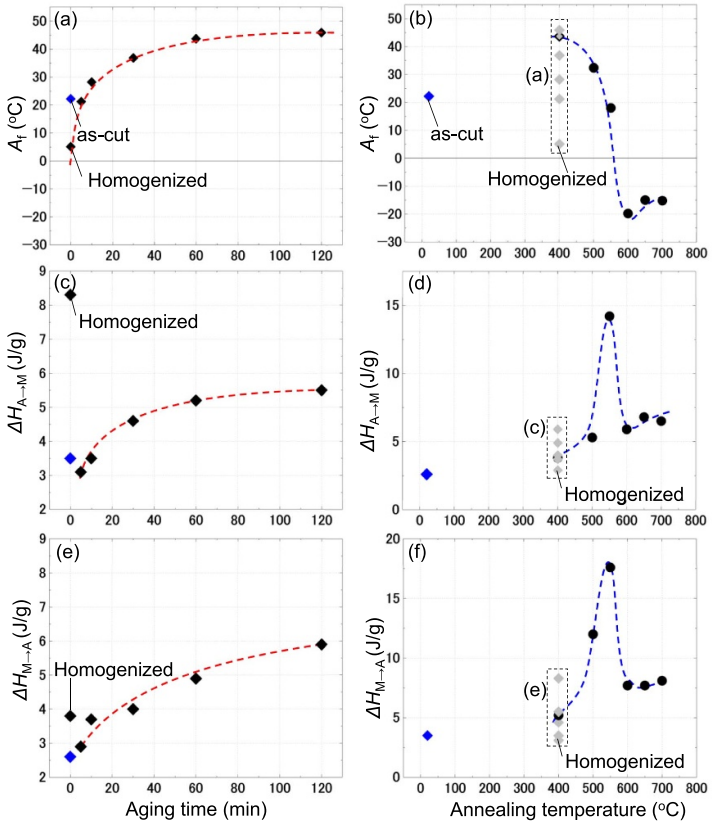

Figure 4. (a), (b) Austenite finish (A_f) temperature and the latent heats (c), (d) $\Delta H_{A\rightarrow M}$ and (e), (f) $\Delta H_{M\rightarrow A}$ obtained from DSC curves for the homogenized sample and samples subsequently aged for 5–120 min at 400 °C and the as-cut sample and heat-treated samples annealed at 400 °C–700 °C for 60 min.

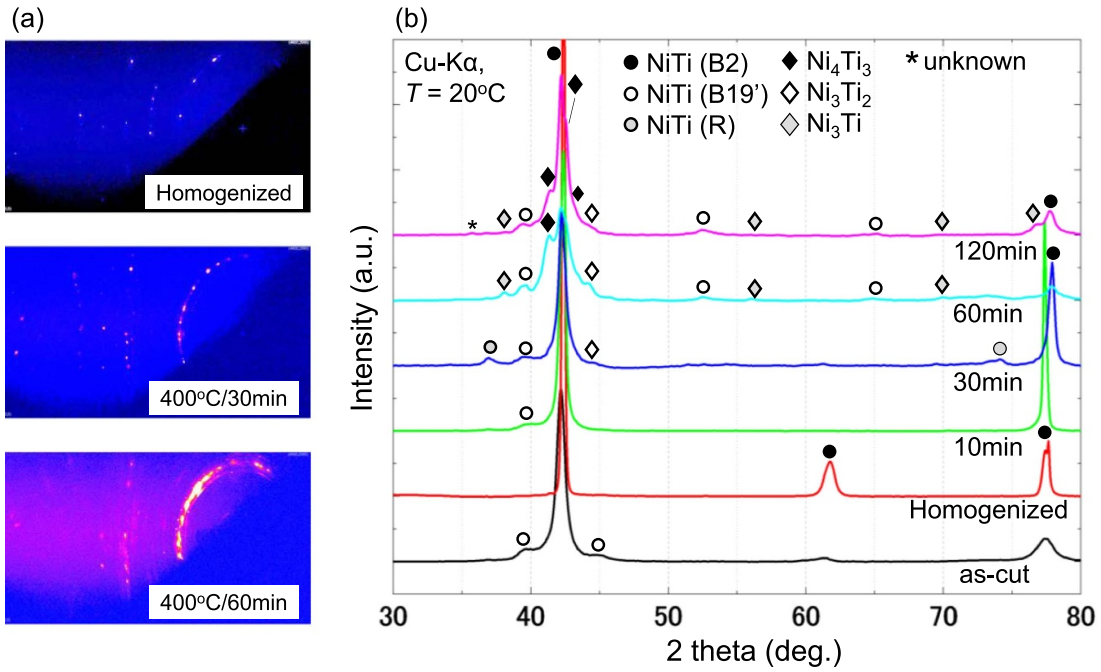

Figure 5. Crystal structure analysis. (a) 2D DeBye-Scherrer XRD images and (b) integrated XRD patterns for as-cut, homogenized, and samples aged for 10, 30, 60, and 120 min at 400 °C.

transformation temperatures to enhance superelasticity. The next step in our work is to design and develop the multi-stage cascade regenerator [6] with multi-A_f materials based on the thermal processing procedures identified in this study.

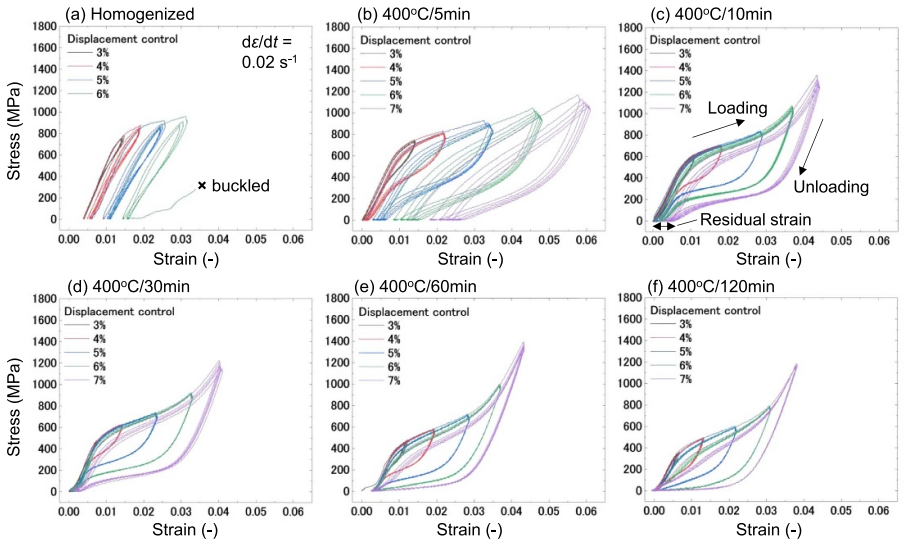

Figure 6. The isothermal stress–strain curves of the superelastic Ni-Ti alloys for (a) homogenizing and annealing at 400 °C aged for (b) 5 min, (c) 10 min, (d) 30 min, (e) 60 min, and (f) 120 min.

3.3. Aging effect on the compressive stress–strain properties

Figure 6 illustrates the aging effect on the superelasticity of Ni-Ti alloys. The homogenized samples displayed limited superelasticity and buckled at 6% applied strain during displacement control. As the aging time period was increased, the plateau stress at which phase transformation began decreased, and the residual strain became smaller (indicating nearly full recovery). When the aging period was 5 min, the residual strain was substantial, indicating that the aging process was inadequate. Conversely, when the aging period was 10 and 30 min, the residual strain was small, and exceptional superelastic properties were observed. An aging treatment of 60 min or longer resulted in very low plateau stress and almost no residual strain in the loading process. The reduced superelasticity was due to the A_f temperature being higher than room temperature (around 20 °C). Also, it is expected that in this instance, the martensitic phase remained in the unloading process without being transformed into the austenitic phase. Furthermore, the strain showing plateau stress was also lower, indicating that the superelastic properties had deteriorated at ambient temperature.

The strain energy generated in the loading/unloading process is from the total volume of phase transformation, and it was highly correlated with the latent heat obtained from the DSC curve. The strain energy, which corresponds to the enclosed area of the stress–strain curve, was found to have a maximum value of 23.8 [MJ m^{-3}] when the aging period was 10 and 30 min. As the residual strain is highly correlated with the cyclical fatigue properties of superelastic materials, the smaller the residual strain, the better the superelastic properties.

3.4. Elastocaloric effect under the adiabatic compression loading/unloading

Figure 7 shows the elastocaloric effect for aged Ni-Ti samples. The adiabatic temperature changes in the loading and unloading process (ΔT_h, ΔT_c) were determined under cyclical compressive stress. As the applied strain was increased from 0.0034 to 0.030, ΔT_h and ΔT_c of the sample aged at 400 °C for 10 min increased (figure 7(b)). The relatively larger temperature lift ΔT_h compared to ΔT_c may be attributed to strain energy loss during the loading and unloading process associated with the austenite-martensite transformation of the Ni-Ti alloy wires [33]. Figure 7(c) illustrates the dependence of ΔT_c on compressive strain for each Ni-Ti tube. The highest value of ΔT_c, 9.4 K, was obtained from the sample aged at 400 °C for 10 min at 3.0% strain.

The thermomechanical properties of Ni-Ti alloy specimens are summarized in table 2. As the aging period increased, the A_f temperature and the $\Delta H_{M \to A}$ increased. The strain energy (E_ε) obtained from the stress–strain loop and the residual strain (ε_{res}) after the last cyclic test was measured as isothermal superelastic properties. It can be observed that ΔT_c is highly correlated with A_f and superelasticity, particularly the shape of the unloading process of stress–strain curves. On the other hand, the maximum temperature change ΔT_h of the sample aged at 400 °C for 60 min showed the largest value of 14.8 K at 3.2% strain. These results indicate that different temperature lifts between ΔT_h and ΔT_c were based on the thermomechanical loss during the hysteresis loop and the difference between martensite start temperatures and austenite start temperatures [34]. Additionally, the relatively low values of temperature lifts of the sample

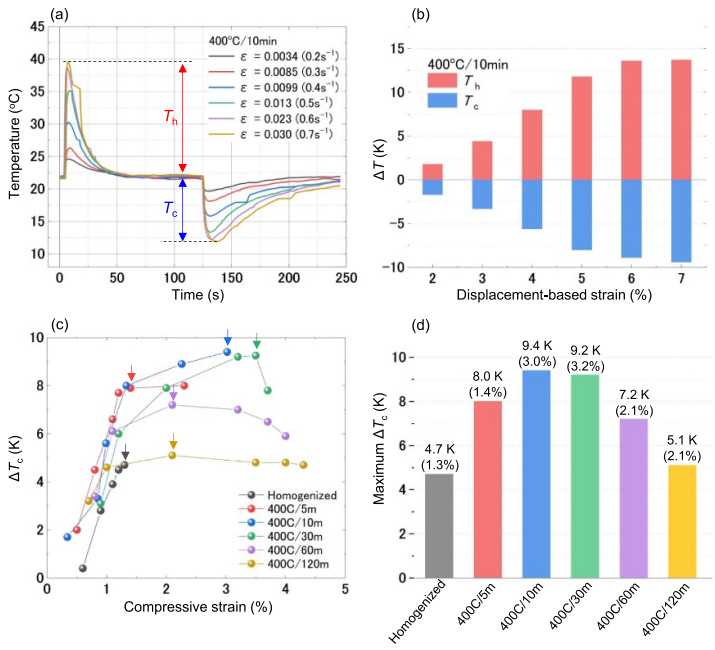

Figure 7. Adiabatic temperature lifts based on elastocaloric effect for aged Ni-Ti samples. (a) Temperature profile as a function of time under cyclic compressive loading and unloading, (b) Temperature changes in the loading (ΔT_h) and unloading (ΔT_c) process, (c) The dependence of ΔT_c on the compressive strain, and (d) the maximum ΔT_c of the Ni-Ti alloys.

Table 2. The thermomechanical properties for homogenized and aged Ni-Ti alloys.

	Superelasticity (isothermal)		Elastocaloric adiabatic temperature lifts	
Samples	Strain energy, E_ε (MJ m^{-3})	Residual strain, ε_{res} (%)	Maximum ΔT_h (K)	Maximum ΔT_c (K)
As-cut	22.3	0.48	14.8	9.3
Homogenized	1.49	N.D.	5.7	4.7
400 °C/5 min	19.4	2.41	11.3	8.0
400 °C/10 min	23.8	0.44	13.7	9.4
400 °C/30 min	23.8	0.26	14.1	9.2
400 °C/60 min	20.7	0.15	14.8	6.5
400 °C/120 min	17.0	0.13	10.5	4.8

aged at 400 °C for 120 min can be attributed to the metallurgical features of Ni-Ti alloys. In particular, the over-aging might have resulted in larger Ni_4Ti_3 precipitates and/or the formation of other Ni-rich intermetallic phases, such as Ni_3Ti_2, which are detrimental to the thermomechanical strength [35, 36]. In terms of the mechanism of elastocaloric cooling, it appears that A_f temperature and $\Delta H_{M \to A}$ affect the temperature lifts ΔT_h and ΔT_c. The result indicates that the A_f temperature should be slightly below the ambient temperature to obtain the higher ΔT_c. These findings suggest that the difference between A_f temperature and ambient temperature can significantly impact the elastocaloric cooling performance.

As per the above results, it was revealed that the as-cut, 400 °C/10 min, 400 °C/30 min, and 400 °C/60 min samples of commercial Ni-Ti tubes exhibited superior elastocaloric cooling at around 3% strain. The A_f temperatures for these samples were found to increase on the order of 22.3 °C, 28.2 °C, 36.8 °C, and 43.7 °C for samples aged for 10, 30, and 60 min, respectively. These findings indicate that thermal treatments have been successful, resulting in the production of Ni-Ti alloys with robust cooling capabilities and a maximum A_f temperature range of 24.7 °C, as determined from the A_f temperature of the samples that were aged for periods between 5–120 min. It is expected that these results will contribute to the development of cascade elastocaloric regenerators with multiple A_f materials.

4. Conclusions

We investigated the impact of thermal processing on commercial $Ni_{50.8}Ti_{49.2}$ alloy tubes in order to understand the correlation between aging treatment and the elastocaloric properties of Ni-Ti alloys. Our results showed that improvement in superelastic properties, such as reduction in residual strain, was

observed as the aging time was increased. Conversely, an increase in A_f temperature resulted in a decrease in elastocaloric temperature lifts. The optimal short-time aging treatment at 400 °C appears to result in good superelasticity and elastocaloric cooling performance with a large tunable austenite finish (A_f) temperature range of 24.7 °C, as determined from the A_f temperature of the samples that were aged for 5–120 min. The exceptional superelasticity might imply the formation of the appropriate amount of Ni_4Ti_3 precipitation in the NiTi matrix phase.

In summary, our work suggests that heat treatment techniques are a valuable tool for fine-tuning the temperature range of superelastic Ni-Ti alloys for elastocaloric cooling. By modifying the microstructure and thermomechanical properties of Ni-Ti alloys, the temperature range of the elastocaloric effect can be adjusted to be more favorable for practical use. We are now actively developing a cascade elastocaloric regenerator incorporating different A_f Ni-Ti tube materials using the procedures we have uncovered in this work.

Data availability statement

All data that support the findings of this study are included within the article (and any supplementary files).

Acknowledgments

The authors acknowledge useful discussions with R Radermacher, Y Hwang, and J Muehlbauer. This work was supported by the U.S. Department of Energy under DE-EE0009159. This work was also supported by Japan Science and Technology Agency, JST/ACT-X (Grant No. JPMJAX22AL), and Japan Society for the Promotion of Science, JSPS (KAKENHI: Grants No. 20K14607 and 19J02078).

ORCID iD

Takahiro Yamazaki https://orcid.org/0000-0003-0738-9373

References

[1] Kabirifar P, Trojer J, Brojan M and Tušek J 2022 From the elastocaloric effect towards an efficient thermodynamic cycle *J. Phys. Energy* **4** 044009
[2] Engelbrecht K 2019 Future prospects for elastocaloric devices *J. Phys. Energy* **1** 021001
[3] Hou H, Qian S and Takeuchi I 2022 Materials, physics and systems for multicaloric cooling *Nat. Rev. Mater.* **7** 20
[4] Greibich F *et al* 2021 Elastocaloric heat pump with specific cooling power of 20.9 W g–1 exploiting snap-through instability and strain-induced crystallization *Nat. Energy* **6** 260–7
[5] Emaikwu N, Catalini D, Muehlbauer J, Hwang Y, Takeuchi I and Radermacher R 2022 Experimental investigation of a staggered-tube active elastocaloric regenerator *Int. J. Refrig.* (https://doi.org/10.1016/j.ijrefrig.2022.09.006)
[6] Ahčin Ž, Liang J, Engelbrecht K and Tušek J 2021 Thermo-hydraulic evaluation of oscillating-flow shell-and-tube-like regenerators for (elasto) caloric cooling *Appl. Therm. Eng.* **190** 116842
[7] Frenzel J, Wieczorek A, Opahle I, Maaß B, Drautz R and Eggeler G 2015 On the effect of alloy composition on martensite start temperatures and latent heats in Ni–Ti-based shape memory alloys *Acta Mater.* **90** 213–31
[8] Otsuka K and Ren X 2005 Physical metallurgy of Ti-Ni-based shape memory alloys *Prog. Mater. Sci.* **50** 511–678
[9] Frenzel J, George E P, Dlouhy A, Somsen C, Wagner M X and Eggeler G 2010 Influence of Ni on martensitic phase transformations in NiTi shape memory alloys *Acta Mater.* **58** 3444–58
[10] Ma J, Karaman I and Noebe R D 2010 High temperature shape memory alloys *Inter. Mater. Rev.* **55** 257–315
[11] Benafan O, Brown J, Calkins F T, Kumar P, Stebner A P, Turner T L, Vaidyanathan R, Webster J and Young M L 2014 Shape memory alloy actuator design: CASMART collaborative best practices and case studies *Int. J. Mech. Mater. Des.* **10** 1–42
[12] Otsuka K and Shimizu K 1986 Pseudoelasticity and shape memory effects in alloys *Int. Met. Rev.* **31** 93–114
[13] Schmidt M, Schütze A and Seelecke S 2016 Elastocaloric cooling processes: the influence of material strain and strain rate on efficiency and temperature span *APL Mater.* **4** 064107
[14] Shahmir H, Nili-Ahmadabadi M and Naghdi F 2011 Superelastic behavior of aged and thermomechanical treated NiTi alloy at Af+ 10 C *Mater. Des.* **32** 365–70
[15] Tušek J and Kitanovski A 2015 Magnetocaloric energy conversion: from theory to applications (https://doi.org/10.1016/j.cmpb.2015.07.008)
[16] Nishida M, Wayman C M and Honma T 1986 Precipitation processes in near-equiatomic TiNi shape memory alloys *Metall. Trans.* A **17** 1505–15
[17] Yan X and Van Humbeeck J 2011 Effect of annealing on strain-temperature response under constant tensile stress in cold-worked NiTi thin wire *Smart Mater. Res.* **2011** 160927
[18] Shamimi A, Amin-Ahmadi B, Stebner A and Duerig T 2018 The effect of low temperature aging and the evolution of R-phase in Ni-rich NiTi *Shape Mem. Superelasticity* **4** 417–27
[19] Girsova S L, Poletika T M and Girsova N V 2020 R-phase transformation in heterogeneous nanocrystalline Ni-rich TiNi alloy *AIP Conf. Proc.* **2310** 020108
[20] Mohamad H, Mahmud A S, Nashrudin M N and Razali M F 2018 Effect of ageing temperatures on pseudoelasticity of Ni-rich NiTi shape memory alloy *AIP Conf. Proc.* **1958** 020008
[21] Huang X and Liu Y 2001 Effect of annealing on the transformation behavior and superelasticity of NiTi shape memory alloy *Scr. Mater.* **45** 153–60

[22] Xu L and Wang R 2010 The effect of annealing and cold-drawing on the super-elasticity of the Ni-Ti shape memory alloy wire *Mod. Appl. Sci.* **4** 109
[23] Fraj B B, Zghal S, Gahbiche A and Tourki Z 2019 Microstructural effect on the thermomechanical behavior of aged Ni-rich NiTi SMA *Mater. Res. Express* **6** 1165c7
[24] Fraj B B, Gahbiche A, Zghal S and Tourki Z 2017 On the influence of the heat treatment temperature on the superelastic compressive behavior of the Ni-rich NiTi shape memory alloy *J. Mater. Eng. Perform.* **26** 5660–8
[25] Feng Y, Gao Z and Hu Z 2022 Influence of annealing treatment on microstructure and properties of Ni-Rich NiTi alloy coating prepared by laser cladding *Materials* **15** 3298
[26] Karimzadeh M, Aboutalebi M R, Salehi M T, Abbasi S M and Morakabati M 2016 Adjustment of aging temperature for reaching superelasticity in highly Ni-rich Ti-51.5 Ni NiTi shape memory alloy *Mater. Manuf. Process.* **31** 1014–21
[27] Young M L, Wagner M X, Frenzel J, Schmahl W W and Eggeler G 2010 Phase volume fractions and strain measurements in an ultrafine-grained NiTi shape-memory alloy during tensile loading *Acta Mater.* **58** 2344–54
[28] Li P, Jia Y, Wang Y, Li Q, Meng F and He Z 2019 Effect of Fe addition on microstructure and mechanical properties of as-cast $Ti_{49}Ni_{51}$ alloy *Materials* **12** 3114
[29] Velmurugan C, Senthilkumar V, Dinesh S and Arulkirubakaran D 2018 Review on phase transformation behavior of NiTi shape memory alloys *Mater. Today* **5** 14597–606
[30] Zhang J, Cai W, Ren X, Otsuka K and Asai M 1999 The nature of reversible change in Ms temperatures of Ti-Ni alloys with alternating aging *Mater. Trans. JIM* **40** 1367–75
[31] Surikov N Y, Panchenko E Y and Chumlyakov Y I 2022 Elastocaloric effect in heterophase TiNi single crystals *Shape Mem. Superelasticity* **8** 226–34
[32] Panchenko E Y, Chumlyakov Y I, Kireeva I V, Ovsyannikov A V, Sehitoglu H, Karaman I and Maier Y H J 2008 Effect of disperse Ti_3N_4 particles on the martensitic transformations in titanium nickelide single crystals *Phys. Met. Metallogr.* **106** 577–89
[33] Cui J, Wu Y, Muehlbauer J, Hwang Y, Radermacher R, Fackler S and Takeuchi I 2012 Demonstration of high efficiency elastocaloric cooling with large ΔT using NiTi wires *Appl. Phys. Lett.* **101** 073904
[34] Cao Y, Zhou X, Cong D, Zheng H, Cao Y, Nie Z, Sun J and Wang Y 2020 Large tunable elastocaloric effect in additively manufactured Ni–Ti shape memory alloys *Acta Mater.* **194** 178–89
[35] Michutta J, Somsen C, Yawny A, Dlouhy A and Eggeler G 2006 Elementary martensitic transformation processes in Ni-rich NiTi single crystals with Ni_4Ti_3 precipitates *Acta Mater.* **54** 3525–42
[36] Kröger A, Dziaszyk S, Frenze J, Somsen C, Dlouhy A and Eggeler G 2010 In-Situ TEM observations of martensitic transformations in Ni-rich NiTi single crystals with coherent and aligned precipitates *Int. Conf. on Martensitic Transformations (ICOMAT)* (Hoboken: Wiley) pp 89–93